Priority Report

Cancer Research

RNA Sequencing Identifies Transcriptionally Viable Gene Fusions in Esophageal Adenocarcinomas

Andrew E. Blum[1], Srividya Venkitachalam[1], Yan Guo[2], Ann Marie Kieber-Emmons[1], Lakshmeswari Ravi[3], Apoorva K. Chandar[4], Prasad G. Iyer[5], Marcia I. Canto[6], Jean S. Wang[7], Nicholas J. Shaheen[8], Jill S. Barnholtz-Sloan[1], Sanford D. Markowitz[9], Joseph E. Willis[10], Yu Shyr[2], Amitabh Chak[4], Vinay Varadan[1], and Kishore Guda[1]

Abstract

Esophageal adenocarcinoma is a deadly cancer with increasing incidence in the United States, but mechanisms underlying pathogenesis are still mostly elusive. In addressing this question, we assessed gene fusion landscapes by comprehensive RNA sequencing (RNAseq) of 55 pretreatment esophageal adenocarcinoma and 49 nonmalignant biopsy tissues from patients undergoing endoscopy for Barrett's esophagus. In this cohort, we identified 21 novel candidate esophageal adenocarcinoma–associated fusions occurring in 3.33% to 11.67% of esophageal adenocarcinomas. Two candidate fusions were selected for validation by PCR and Sanger sequencing in an independent set of pretreatment esophageal adenocarcinoma ($N = 115$) and nonmalignant ($N = 183$) biopsy tissues. In particular, we observed RPS6KB1–VMP1 gene fusion as a recurrent event occurring in approximately 10% of esophageal adenocarcinoma cases. Notably, esophageal adenocarcinoma cases harboring RPS6KB1–VMP1 fusions exhibited significantly poorer overall survival as compared with fusion-negative cases. Mechanistic investigations established that the RPS6KB1–VMP1 transcript coded for a fusion protein, which significantly enhanced the growth rate of nondysplastic Barrett's esophagus cells. Compared with the wild-type VMP1 protein, which mediates normal cellular autophagy, RPS6KB1–VMP1 fusion exhibited aberrant subcellular localization and was relatively ineffective in triggering autophagy. Overall, our findings identified RPS6KB1–VMP1 as a genetic fusion that promotes esophageal adenocarcinoma by modulating autophagy-related processes, offering new insights into the molecular pathogenesis of esophageal adenocarcinomas. *Cancer Res; 76(19); 5628–33. ©2016 AACR.*

Introduction

The incidence of esophageal adenocarcinoma has increased rapidly in the past few decades while remaining a highly morbid and mortal disease (1). In fact, esophageal adenocarcinoma is now the most common esophageal malignancy in the United States. Despite the recognition of Barrett's esophagus as a premalignant condition, mechanisms underlying esophageal adenocarcinoma progression remain unclear (2). Somatic gene fusions in cancers are being increasingly recognized for their potential tumorigenic roles across malignancies and can be attractive as diagnostic and therapeutic molecular targets. Here, we used whole-transcriptome RNA sequencing (RNAseq) to map and characterize transcriptionally viable gene fusions on a genome scale in esophageal adenocarcinomas.

Materials and Methods

Detailed methods are provided in Supplementary Materials and Methods.

Patient samples

We compiled a discovery set of 109 samples for RNAseq, consisting of 55 pretreatment esophageal adenocarcinomas, 49 nonmalignant tissue samples, and 5 esophageal adenocarcinoma cell lines. We also compiled an independent validation set ($N = 298$) of 115 pretreatment esophageal adenocarcinomas and 183 normal/nonmalignant tissue samples.

Survival analysis

Kaplan–Meier plots and survival differences were estimated using the Peto–Prentice test (3).

[1]Division of General Medical Sciences-Oncology, Case Comprehensive Cancer Center, Case Western Reserve University, Cleveland, Ohio. [2]Center for Quantitative Sciences, Vanderbilt Ingram Cancer Center, Nashville, Tennessee. [3]Division of Hematology and Oncology, Case Comprehensive Cancer Center, Case Western Reserve University, Cleveland, Ohio. [4]Division of Gastroenterology, Case Comprehensive Cancer Center, Case Western Reserve University, Cleveland, Ohio. [5]Barrett's Esophagus Unit, Division of Gastroenterology and Hepatology, Mayo Clinic, Rochester, Minnesota. [6]Division of Gastroenterology and Hepatology, Department of Medicine, The Johns Hopkins Medical Institutions, Baltimore, Maryland. [7]Division of Gastroenterology, Department of Medicine, Washington University School of Medicine, St. Louis, Missouri. [8]Division of Gastroenterology and Hepatology, Center for Esophageal Diseases and Swallowing, University of North Carolina, Chapel Hill, North Carolina. [9]Department of Medicine, Case Comprehensive Cancer Center, Case Western Reserve University, Cleveland, Ohio. [10]Department of Pathology, Case Comprehensive Cancer Center, Case Western Reserve University, Cleveland, Ohio.

Note: Supplementary data for this article are available at Cancer Research Online (http://cancerres.aacrjournals.org/).

A.E. Blum and S. Venkitachalam contributed equally to this article.

Corresponding Author: Kishore Guda, Case Comprehensive Cancer Center, Case Western Reserve University, 2103 Cornell Rd, WRB-3143, Cleveland, OH 44106. Phone: 216-368-5665; Fax: 216-368-8928; E-mail: kkg5@case.edu

doi: 10.1158/0008-5472.CAN-16-0979

AACR

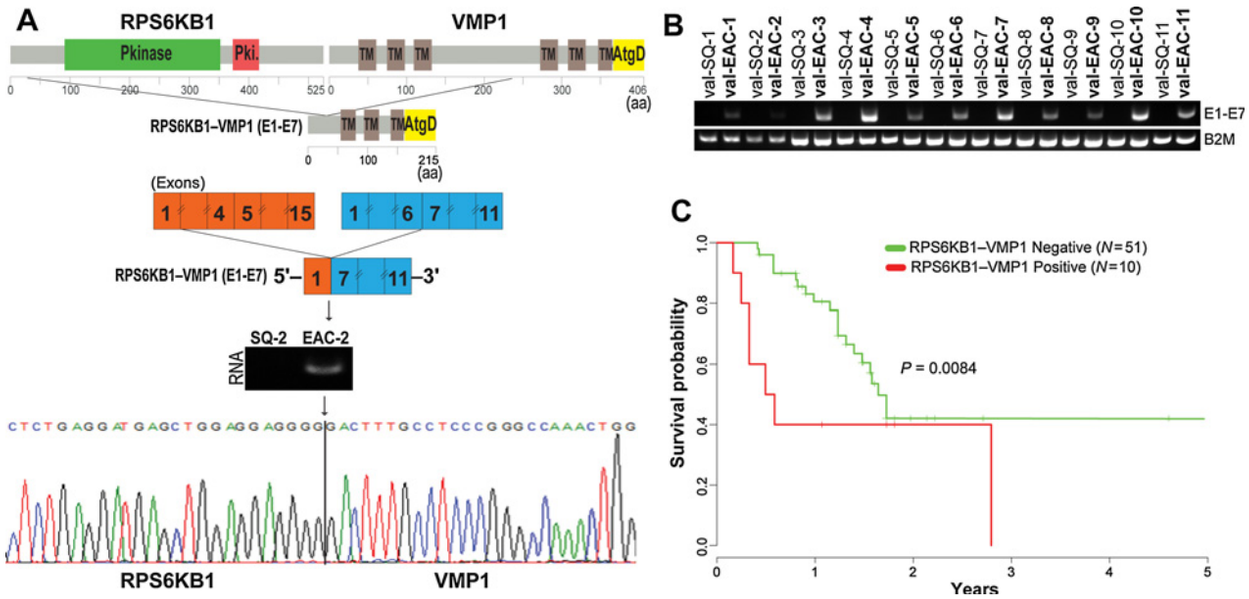

Figure 1.

RPS6KB1–VMP1 fusion in esophageal adenocarcinoma (EAC). **A,** top, conserved protein domains in RPS6KB1 and VMP1, along with their length in amino acids (aa); middle, native gene exons included in the RPS6KB1–VMP1 fusion transcript; bottom, PCR-amplified product spanning the E1-E7 isoform of the RPS6KB1–VMP1 fusion junction, along with the Sanger sequencing chromatogram of the fusion junction in representative esophageal adenocarcinoma and matched subcutaneous (SQ) tissues used in the discovery RNAseq study. **B,** representative agarose gel images of RPS6KB1–VMP1 (E1-E7) fusion junction PCR product from matched normal squamous and fusion-positive primary esophageal adenocarcinoma tissue RNAs ($N = 11$ pairs), included in the validation (val) cohort. β-2 microglobulin (B2M) was used as an endogenous RNA control. **C,** Kaplan–Meier survival curves for stage III esophageal adenocarcinomas with or without the RPS6KB1–VMP1 (E1-E7) fusion.

Whole-genome sequencing

Whole-genome sequencing was performed on FLO-1 cell line DNA. BreakDancer (4) was used to identify for structural/copy-number aberrations in the vicinity of the RPS6KB1–VMP1 fusion breakpoint.

Copy-number assay

Primary tissue DNAs were evaluated for copy-number alterations using TaqMan assay for genes in the vicinity of the RPS6KB1–VMP1 fusion breakpoint.

Cell lines

Cell lines were obtained as follows: Cos7 and CP-A cells (ATCC), HEK-293FT (Life Technologies), FLO-1 and SKGT4 (kindly provided by Dr. Navtej Buttar, Mayo Clinic), JH-EsoAd1 (kindly provided by Drs. James Eshleman and Anirban Maitra, Johns Hopkins University School of Medicine, Baltimore, MD), OE19 and OE33 (Sigma). All cell lines were obtained in 2014 and tested for authenticity using STR genotyping and were screened periodically for mycoplasma contamination.

Generation of stable CP-A cells

CP-A cells were infected with replication-deficient lentivirus to stably express full-length RPS6KB1–VMP1 (E1-F7, E4-E7) fusion, or β-tubulin class I (TUBB) control transcript.

Cell growth assay

CP-A cells, stably expressing each of the fusion or control gene transcripts, were assessed for growth over a course of 120 hours following seeding using the automated IncuCyte system.

Colocalization analysis of LC3A/B with RPS6KB1–VMP1 and VMP1 proteins

Cos7 cells, carrying empty vector, or V5-His containing full-length RPS6KB1–VMP1 or VMP1 transcript, were incubated with anti-microtubule–associated protein 1 light chain 3 (LC3B) and anti-V5 antibodies, followed by incubation with Alexa-conjugated secondary antibodies and imaging using a Leica SP8 super resolution confocal microscope.

Coimmunoprecipitation of Beclin1 with RPS6KB1–VMP1 and VMP1 proteins

Total cell lysates from Cos7 cells, carrying empty vector or V5-His containing full-length RPS6KB1–VMP1 or VMP1 transcript, were immunoprecipitated using anti-V5 agarose beads. Western blots were performed with anti-V5 HRP and anti-Beclin1 antibodies.

Western blot analysis of LC3A/B

Cos7 and CP-A cells expressing full-length RPS6KB1–VMP1 or VMP1 or vector/baseline control transcripts were grown in nutrient-depleted medium and subsequently treated with 30 μmol/L chloroquine for 4 hours at 37°C. LC3A/B protein expression was subsequently assessed by Western blot analysis using anti-LC3A/B antibody.

Results and Discussion

Discovery of candidate gene fusions in esophageal adenocarcinomas

We used the deFuse algorithm (5) to detect putative gene fusions in esophageal adenocarcinoma and nonmalignant

tissues, included in the RNAseq discovery sample set (Supplementary Tables S1–S3). We identified 23 candidate esophageal adenocarcinoma–associated fusion transcripts, retaining an open reading frame and occurring in 3.33% to 11.67% of esophageal adenocarcinomas (Supplementary Table S4), of which 21 (91%) were confirmed by PCR and Sanger sequencing analyses of the fusion junctions in respective samples (Supplementary Table S4), likely suggesting a false-positive rate of 9% in the informatics-based discovery in this study. Next, of these 21 PCR-confirmed candidate fusions, we prioritized two fusions, OSBPL1A (oxysterol-binding protein–like 1A)–LAMA3 (laminin alpha 3), and RPS6KB1 (ribosomal protein S6 kinase)–VMP1 (vacuole membrane protein 1; Supplementary Fig. S1) for further studies based on the following criteria: we compared the 23 fusions from our study with prior whole-genome DNA sequencing studies in esophageal adenocarcinomas reporting on structural variants (6, 7) and found fusions affecting the *LAMA3* gene to be common across the two prior studies (6, 7) and our current study. On the other hand, RPS6KB1–VMP1 fusion had been previously described in breast cancers, where its expression was found to be associated with poorer survival in breast cancer patients (8). Accordingly, we prioritized OSBPL1A–LAMA3 and RPS6KB1–VMP1 for further validation analysis. Of note, two versions of RPS6KB1–VMP1 fusion (E1-E7 and E4-E7) were identified (Supplementary Fig. S1) by deFuse and/or by PCR-based cloning in the discovery esophageal adenocarcinoma samples, both of which lacked the full RPS6KB1 kinase domain and encoded a truncated VMP1 protein.

RPS6KB1–VMP1 is a recurrent fusion in esophageal adenocarcinomas with prognostic potential

Assessment of the two candidate fusions using PCR and Sanger sequencing in an independent set of esophageal adenocarcinoma ($N = 115$) and normal/nonmalignant ($N = 183$) tissues (Supplementary Table S5) revealed RPS6KB1–VMP1 (E1-E7) as a recurrent fusion present in 9.56% of esophageal adenocarcinomas but not detectable in normal/nonmalignant tissue samples (Supplementary Table S6; Fig. 1B). On the other hand, the E4-E7 RPS6KB1–VMP1 isoform and the OSBPL1A–LAMA3 fusions were not detected in any of the esophageal adenocarcinomas (Supplementary Table S6) or in the normal/nonmalignant tissues in the validation cohort.

We next evaluated the clinical significance of the RPS6KB1–VMP1 (E1-E7) fusion by assessing its association with overall survival in stage III esophageal adenocarcinoma patients. Esophageal adenocarcinoma patients harboring RPS6KB1–VMP1 fusion exhibited significantly poorer overall survival than fusion-negative patients (Fig. 1C, $P = 0.0084$), consistent with the findings in breast cancer (8). In addition, the overall survival of fusion-positive esophageal adenocarcinoma patients remained poor even after adjusting for age at diagnosis and tumor grade using a Cox proportional hazards model ($P = 0.051$), highlighting the prognostic potential of this fusion.

Potential genomic mechanisms underlying RPS6KB1–VMP1 fusion

VMP1 and *RPS6KB1* genes are both localized on the same strand on chromosome 17q23.1, with *VMP1* gene located 5′ to the *RPS6KB1* gene. Given that VMP1 is the 3′ partner of the RPS6KB1–VMP1 fusion (Fig. 1A), it is unlikely that transcription read-through or transsplicing may be the underlying causative mechanism of this fusion. Indeed, the deFuse algorithm suggests this fusion could be a consequence of genomic rearrangements in the chromosome 17q23.1 region (Supplementary Table S2), likely resulting from tandem DNA duplications in this chromosomal locus. Interestingly, copy-number aberrations, a consequence of such tandem duplication events, are frequently observed in chromosome 17q in esophageal adenocarcinomas (9, 10). Consistent with this, whole-genome DNA sequencing in the RPS6KB1–VMP1 expressing FLO-1 (EAC-48) cell line revealed copy-number gains in the vicinity of *RPS6KB1* and *VMP1* genes (Supplementary Fig. S2). Additional qPCR-based copy-number analysis in a set ($N = 10$) of fusion-positive primary esophageal adenocarcinomas also revealed significant copy-number gains in 17q23.1 genomic locus, accounting for 40% of esophageal adenocarcinomas tested (Supplementary Fig. S2). These findings, taken together with the prior report in breast cancer (8), strongly suggest that genomic rearrangements, potentially resulting from tandem duplications in the 17q23 locus, facilitate fusion between

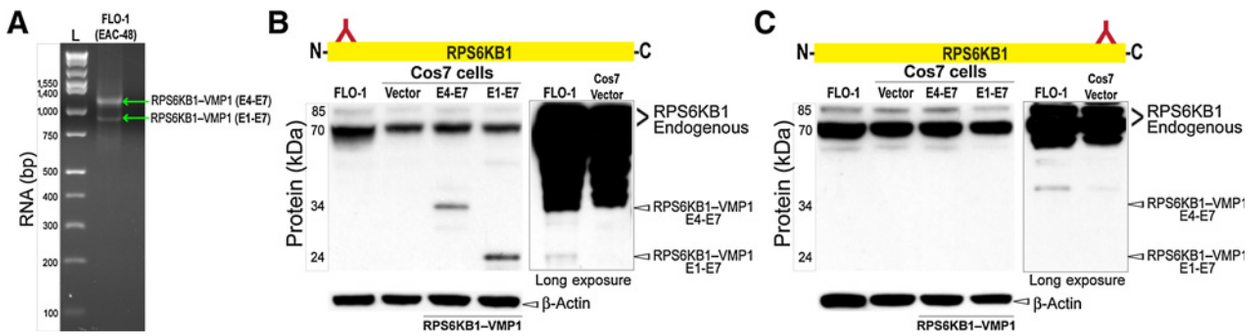

Figure 2.

Assessing the protein-coding potential of RPS6KB1–VMP1 fusion in mammalian cells. **A,** representative gel image showing the expression of full-length RPS6KB1–VMP1 fusion transcripts (E1-E7 and E4-E7) in FLO-1 cell line RNA. L, DNA ladder. **B,** Western blot analysis using an N-terminal (inverted Y) anti-RPS6KB1 primary antibody in FLO-1 and Cos7 cells ectopically expressing full-length RPS6KB1–VMP1 fusion transcripts or vector; right, radiographic image of FLO-1 and vector-carrying Cos7 cells at approximately 5-minute exposure (long exposure). **C,** Western blot analysis using a negative control C-terminal (inverted Y) anti-RPS6KB1 primary antibody in Cos7 and FLO-1 cells from above showing no detection of the fusion protein.

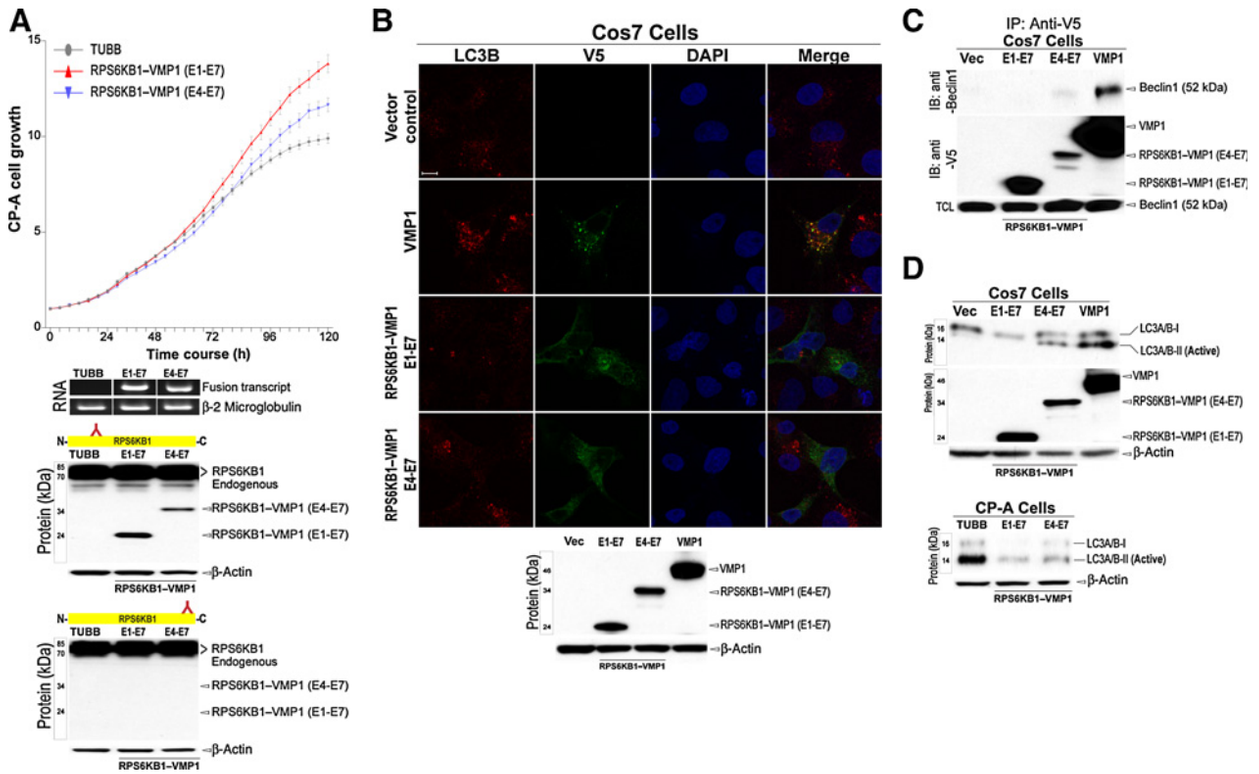

Figure 3.

Functional characterization of the RPS6KB1–VMP1 fusion. **A,** top, effect of RPS6KB1–VMP1 fusion transcripts on CP-A cell growth. The *y*-axis represents the average confluence values of two independently derived stable clones per experimental arm, with 12 replicates each, normalized to time zero (*x*-axis). Error bars, SEM. Bottom, PCR analyses of fusion transcripts in RNA derived from CP-A cells transfected with control gene (TUBB) or fusion transcripts and Western blot analysis demonstrating fusion protein detection with the N-terminal anti-RPS6KB1 antibody. **B,** top, localization of ectopically expressed RPS6KB1–VMP1 and VMP1 proteins in Cos7 cells, detected by anti-V5 antibody (green fluorescence), and endogenous LC3B protein, a marker of autophagosome (red fluorescence). Note the diffuse staining pattern of RPS6KB1–VMP1 fusion protein, as opposed to the specific colocalization of VMP1 with LC3B protein (scale bar, 10 μm). Bottom, Western blot analysis demonstrating the protein expression of ectopically expressed VMP1 and RPS6KB1–VMP1 fusion in Cos7 cells. **C,** immunoprecipitation (IP) and immunoblotting (IB) analysis in Cos7 cells demonstrating the lack of interaction of RPS6KB1–VMP1 (E1-E7) fusion protein with Beclin1, as compared with the RPS6KB1–VMP1 (E4-E7) fusion or VMP1 protein. Western blot analysis demonstrates equivalent amounts of endogenous Beclin1 protein present in Cos7 total cell lysates (TCL) across treatment groups. **D,** top, Western blot analysis using anti-LC3A/B antibody in Cos7 cells, following nutrient depletion and chloroquine treatment, showing significant induction of LC3A/B-II product in VMP1-expressing cells, as compared with Cos7 cells carrying the RPS6KB1–VMP1 (E1-E7) fusion. Also, note the reduction in the protein levels of LC3A/B-I in RPS6KB1–VMP1 (E1-E7)–expressing cells as compared with vector control. Western blot analysis demonstrates protein expression of ectopically expressed VMP1 and RPS6KB1–VMP1 fusion transcripts in Cos7 cells. Bottom, Western blot analysis using anti-LC3A/B antibody in CP-A cells, stably expressing RPS6KB1–VMP1 fusion or control TUBB transcripts, after nutrient depletion and chloroquine treatment. Note the significant induction of LC3A/B-II product in TUBB-expressing CP-A cells, as compared with the CP-A cells carrying the RPS6KB1–VMP1 (E1-E7) fusion.

RPS6KB1 and *VMP1* in a subset of fusion-positive esophageal adenocarcinomas.

Protein-coding potential of RPS6KB1–VMP1 fusion transcript

We evaluated whether the RPS6KB1–VMP1 transcript indeed codes for protein or represents a noncoding fusion transcript. To test this, we performed Western blot analyses in Cos7 cells ectopically expressing the E1-E7 and E4-E7 fusion transcripts, and in FLO-1 cells endogenously expressing the fusion transcripts (Fig. 2A), using specific antibodies against N- and C-terminal regions of the native RPS6KB1 protein. As expected, while the endogenous RPS6KB1 protein was detected using either N- or C-terminal anti-RPS6KB1 antibodies, only the N-terminal antibody detected the fusion protein (Fig. 2B and C) in these cells. Taken together, these findings suggest that the RPS6KB1–VMP1 transcript can code for a fusion protein in mammalian cells. We nonetheless note that the low levels of the endogenous fusion protein observed in the FLO-1 cells (Fig. 2B) is consistent with the relatively low observed RNA read counts of the RPS6KB1–VMP1 fusion isoforms in the FLO-1 cell line (Supplementary Table S2).

Functional characterization of RPS6KB1–VMP1 fusion

Assessment of transforming potential of RPS6KB1–VMP1 (E1-E7) using the standard NIH/3T3 model did not reveal this fusion as inducing neoplastic transformation (Supplementary Fig. S3). This is in line with prior studies suggesting that many of the gene fusions identified in tumors are not sufficient to drive malignant transformation *per se* and that additional genomic aberrations are likely required for neoplastic transformation (11). Given that the RPS6KB1–VMP1 fusion is detected in the FLO-1 esophageal adenocarcinoma cell line, we also attempted to

evaluate whether knockdown of the fusion transcript in FLO-1 impairs anchorage-independent growth. However, repeated attempts to design and induce siRNA-mediated knockdown of the RPS6KB1–VMP1 fusion transcript in FLO-1 cells were technically unsuccessful. Therefore, as an alternative approach, we proceeded to functionally characterize this fusion using a widely employed nondysplastic Barrett's esophagus cell line model (CP-A), especially given that the vast majority of esophageal adenocarcinomas arise from Barrett's esophagus.

We found CP-A cells stably expressing the RPS6KB1–VMP1 (E1-E7) fusion isoform to exhibit a significant increase in growth rate ($P < 0.001$), which was evident at higher cell densities during the later time points (Fig. 3A). As high cell density has been shown to be a potent inducer of cellular autophagy (12, 13), and RPS6KB1–VMP1 encodes a truncated VMP1, a well-known autophagy-inducing protein (14), we hypothesized that this fusion may be defective in triggering cellular autophagy. We accordingly proceeded to assess the potential effects of this fusion on cellular autophagy processes. Given that VMP1 triggers the formation of autophagosmomes by recruiting LC3 (14), we speculated that the RPS6KB1–VMP1 fusion with a truncated VMP1 may not colocalize with LC3/autophagosomes. Indeed, as shown in Fig. 3B, while VMP1 exhibited striking colocalization with LC3B as distinct punctae, RPS6KB1–VMP1 fusion proteins showed a diffuse localization pattern. In line with this, coimmunoprecipitation studies revealed the RPS6KB1–VMP1 (E1-E7) fusion as neither exhibiting interaction with Beclin1 (Fig. 3C), another key promoter of autophagy (14, 15), nor inducing LC3A/B-II protein expression, a marker of active autophagy processes (15), in Cos 7 cells. This finding was independently confirmed in nutrient-deprived CP-A cells, where TUBB showed a marked induction of the active LC3A/B-II protein, as compared with the RPS6KB1–VMP1 (E1-E7) fusion isoform (Fig. 3D). Incidentally, our observation of tubulin as a potent inducer of active LC3A/B-II protein (Fig. 3D) is in line with its known role in stimulating autophagy under nutrient-deprived conditions (16). Also interestingly, cells expressing the RPS6KB1–VMP1 (E1-E7) isoform exhibited reduced levels of LC3A/B-I protein when compared with the controls (Fig. 3D), suggesting that the E1-E7 fusion may additionally exert dominant negative effects on cellular autophagy processes. Taken together, these findings suggest that the RPS6KB1–VMP1 fusion may play a role in esophageal adenocarcinoma pathogenesis via impairing cellular autophagy, resulting either from VMP1 haploinsufficiency and/or due to dominant negative effects of the E1-E7 fusion on cellular autophagy processes. Further studies are warranted to delineate the timing and significance of autophagy pathway deregulations during esophageal adenocarcinoma pathogenesis.

In summary, our study provides genome-scale characterization of transcriptionally viable gene fusions in esophageal adenocarcinomas. Intriguingly, apart from the candidate esophageal adenocarcinoma–associated fusions listed in Supplementary Table S4, our RNAseq informatics analysis also detected additional fusions that were present in both esophageal adenocarcinoma and matched normal squamous tissues but not in normal gastric or unmatched Barrett's esophagus tissues in the RNAseq dataset (Supplementary Table S7). While we did not prioritize such fusions in this study nor did we determine whether these are selectively occurring in squamous tissue derived from patients with cancer, deciphering the role of these additional fusions in esophageal adenocarcinoma pathogenesis and their potential utility as early biomarkers of disease progression clearly warrants separate investigation.

Disclosure of Potential Conflicts of Interest

V. Varadan is a consultant/advisory board member for Curis, Inc. No potential conflicts of interest were disclosed by the other authors.

Authors' Contributions

Conception and design: A.E. Blum, S.D. Markowitz, V. Varadan, K. Guda
Development of methodology: A.E. Blum, K. Guda
Acquisition of data (provided animals, acquired and managed patients, provided facilities, etc.): A.E. Blum, S. Venkitachalam, A.K. Chandar, P.G. Iyer, M.I. Canto, J.S. Wang, N.J. Shaheen, J.E. Willis, A. Chak, K. Guda
Analysis and interpretation of data (e.g., statistical analysis, biostatistics, computational analysis): A.E. Blum, Y. Guo, J.S. Barnholtz-Sloan, J.E. Willis, Y. Shyr, V. Varadan, K. Guda
Writing, review, and/or revision of the manuscript: A.E. Blum, P.G. Iyer, J.S. Wang, N.J. Shaheen, J.S. Barnholtz-Sloan, A. Chak, V. Varadan, K. Guda
Administrative, technical, or material support (i.e., reporting or organizing data, constructing databases): A.E. Blum, A.M. Kieber-Emmons, L. Ravi, A.K. Chandar, J.S. Wang, A. Chak, K. Guda
Study supervision: A.E. Blum, K. Guda

Acknowledgments

We thank Graham Wiley at the OMRF for performing RNA sequencing. We thank Dr. John P. Lynch at the University of Pennsylvania for his valuable suggestions on propagating CP-A cells. We thank Wendy Brock, Hilary Cosby, Thomas Hollander, and Susan Moist for their efforts in recruiting subjects and coordinating the accrual of samples.

Grant Support

This research was supported by PHS awards: K08 CA148980 (K. Guda), R01 CA204549 (K. Guda), U01 CA152756 (K. Guda and S.D. Markowitz), U54 CA163060 (to all authors), Career Development Program of Case GI SPORE (P50 CA150964) awards (K. Guda and V. Varadan), Case GI SPORE P50 CA150964 (S.D. Markowitz, J.S. Barnholtz-Sloan, J.E. Willis, A. Chak, and K. Guda), R25T CA094186 (V. Varadan), DK083251 (A.E. Blum and A.M. Kieber-Emmons), K24 DK100548 (N.J. Shaheen), P30 DK034987 (N.J. Shaheen), P30 DK89502 (M.I. Canto), and P30 CA043703 (K. Guda, V. Varadan, S.D. Markowitz, J.S. Barnholtz-Sloan, and J.E. Willis), and P30 DK097948 (V. Varadan)

Received April 7, 2016; revised July 10, 2016; accepted July 19, 2016; published OnlineFirst August 8, 2016.

References

1. Hur C, Miller M, Kong CY, Dowling EC, Nattinger KJ, Dunn M, et al. Trends in esophageal adenocarcinoma incidence and mortality. Cancer 2013;119:1149–58.
2. Spechler SJ, Souza RF. Barrett's esophagus. N Engl J Med 2014;371:836–45.
3. Yang S, Prentice R. Improved logrank-type tests for survival data using adaptive weights. Biometrics 2010;66:30–8.
4. Chen K, Wallis JW, McLellan MD, Larson DE, Kalicki JM, Pohl CS, et al. BreakDancer: an algorithm for high-resolution mapping of genomic structural variation. Nat Methods 2009;6:677–81.

5. McPherson A, Hormozdiari F, Zayed A, Giuliany R, Ha G, Sun MG, et al. deFuse: an algorithm for gene fusion discovery in tumor RNA-Seq data. PLoS Comput Biol 2011;7:e1001138.
6. Dulak AM, Stojanov P, Peng S, Lawrence MS, Fox C, Stewart C, et al. Exome and whole-genome sequencing of esophageal adenocarcinoma identifies recurrent driver events and mutational complexity. Nat Genet 2013; 45:478–86.
7. Nones K, Waddell N, Wayte N, Patch AM, Bailey P, Newell F, et al. Genomic catastrophes frequently arise in esophageal adenocarcinoma and drive tumorigenesis. Nat Commun 2014;5: 5224.
8. Inaki K, Hillmer AM, Ukil L, Yao F, Woo XY, Vardy LA, et al. Transcriptional consequences of genomic structural aberrations in breast cancer. Genome Res 2011;21:676–87.
9. El-Rifai W, Harper JC, Cummings OW, Hyytinen ER, Frierson HFJr, Knuutila S, et al. Consistent genetic alterations in xenografts of proximal stomach and gastro-esophageal junction adenocarcinomas. Cancer Res 1998;58:34–7.
10. Miller CT, Moy JR, Lin L, Schipper M, Normolle D, Brenner DE, et al. Gene amplification in esophageal adenocarcinomas and Barrett's with high-grade dysplasia. Clin Cancer Res 2003;9:4819–25.
11. Mitelman F, Johansson B, Mertens F. The impact of translocations and gene fusions on cancer causation. Nat Rev Cancer 2007;7:233–45.
12. Levine B, Yuan J. Autophagy in cell death: an innocent convict? J Clin Invest 2005;115:2679–88.
13. Pattingre S, Levine B. Bcl-2 inhibition of autophagy: a new route to cancer? Cancer Res 2006;66:2885–8.
14. Ropolo A, Grasso D, Pardo R, Sacchetti ML, Archange C, Lo Re A, et al. The pancreatitis-induced vacuole membrane protein 1 triggers autophagy in mammalian cells. J Biol Chem 2007;282:37124–33.
15. Mizushima N, Yoshimori T, Levine B. Methods in mammalian autophagy research. Cell 2010;140:313–26.
16. Geeraert C, Ratier A, Pfisterer SG, Perdiz D, Cantaloube I, Rouault A, et al. Starvation-induced hyperacetylation of tubulin is required for the stimulation of autophagy by nutrient deprivation. J Biol Chem 2010;285: 24184–94.